

Conduction-Electron Resonance Linewidth in Dilute Magnetic Alloys above the Kondo Critical Field at Very Low Temperatures*

B. GIOVANNINI AND R. ORBACH

Physics Department, University of California, Los Angeles, California 90024

(Received 8 July 1970)

The zero-temperature transverse dynamic susceptibility at frequency Ω , $\chi_e^-(\Omega)$, is calculated diagrammatically for conduction electrons in a dilute magnetic alloy. The static magnetic field is assumed to be sufficiently large to quench the Kondo divergence. The exchange interaction is treated to second order in the coupling constant J . It is found that the conduction-electron magnetic-resonance response is a δ function at the exchange-“dressed” conduction-electron resonance frequency ω_e' , with a superimposed Lorentzian envelope centered at ω_e' , which is finite (“turns on”) at frequencies $\Omega > \omega_s$, where ω_s is the localized spin resonance frequency. The implications of this result are discussed with reference to the magnetic-resonance bottleneck, and previous (approximate) calculations of the zero-temperature magnetic-resonance response.

I. INTRODUCTION

Heretofore, attention has been focused primarily on the magnetic-resonance properties of only the localized spin in dilute magnetic alloys.¹ It is the purpose of this paper to exhibit a result for the $T=0$ transverse dynamic spin susceptibility of the conduction-electron spins for a dilute ($c \ll 1$) alloy, to second order in the exchange interaction

$$\mathcal{H}_I = - (J/N) \sum_{\mathbf{q}, j} e^{-i\mathbf{q} \cdot \mathbf{R}_j} \mathbf{S}_j \cdot \boldsymbol{\sigma}_{\mathbf{q}}, \quad (1)$$

where J is the exchange coupling constant, \mathbf{S}_j the spin of the localized moment at position \mathbf{R}_j , and $\boldsymbol{\sigma}_{\mathbf{q}}$ the \mathbf{q} th spatial Fourier component of the conduction-electron spin $\boldsymbol{\sigma}(\mathbf{r})$. This quantity has been computed already, but with the use of decoupling techniques.^{2,3} In these calculations, not only were the usual decoupling approximations made, but also a somewhat artificial separation was made of operators which allowed an exchange self-energy to be defined at all. By examining the structure of the imaginary part of the one-electron self-energy—in particular, the spin-flip part (the only finite contribution at zero temperature)—we have been able to compute the effective zero-temperature width of the conduction-electron magnetic-resonance line. As will be shown in Sec. II, the result is a resonance response which is a rapidly varying function of frequency. The response function consists of a δ function at the exchange-shifted conduction-electron resonance line position, and a superimposed asymmetric “Lorentzian” line centered at the same position, but of finite amplitude only when the external frequency Ω exceeds the localized spin Zeeman frequency ω_s . This surprising result turns out to be mirrored somewhat in the decoupling result of Refs. 2 and 3, as exhibited in Sec. III.

Such a rapid frequency variation of the conduction-electron resonance linewidth has implications for the so-called “magnetic-resonance bottleneck” problem. In

particular, at very low temperatures it would appear that the bottleneck would essentially be absent for $\Omega < \omega_s$ and in full force for $\Omega > \omega_s$. This could lead to sharply asymmetric resonance line shapes for the localized-spin-dominated bottlenecked resonance, as well as for conduction-electron spin resonance itself. The implications are discussed in detail in Sec. III.

Finally, we emphasize that we are ignoring Kondo-like divergences. That is, we are assuming that the static magnetic field H_0 is large compared to the “critical” Kondo field $H_c \sim (D/2\mu) e^{-1/\rho J}$, where a rectangular approximation (magnitude ρ , centered at E_F , and width $2D$) has been made for the conduction-electron density of states.

II. $T=0$ CONDUCTION-ELECTRON TRANSVERSE DYNAMIC SUSCEPTIBILITY

A number of previous calculations^{4,5} exist for the self-energy of a conduction electron interacting with a random array of localized spins (assumed to be in equilibrium with the lattice) via the exchange interaction (1). Abrikosov’s diagrammatic calculation did not include the magnetic-resonance response function. Spencer’s diagrammatic calculation⁵ was carried out for all temperatures (but explicitly presented only for equal g factors, i.e., for $\omega_e = \omega_s$). The work of Orbach and Spencer² was applicable to all temperatures and displayed for arbitrary g factors, but utilized a decoupling scheme. By virtue of this approximation, they were able to compute the full dynamic transverse susceptibility for a coupled localized conduction-electron system (neglecting vertex corrections for the conduction electrons). We shall compare their results at $T=0$ with the exact results of this section in Sec. III.

If Spencer’s diagrammatic method is applied to a dilute alloy for $\omega_e \neq \omega_s$, one finds, using (1) at zero temperature, the following second-order exchange self-energies for “up” (\uparrow) and “down” (\downarrow) spins in a

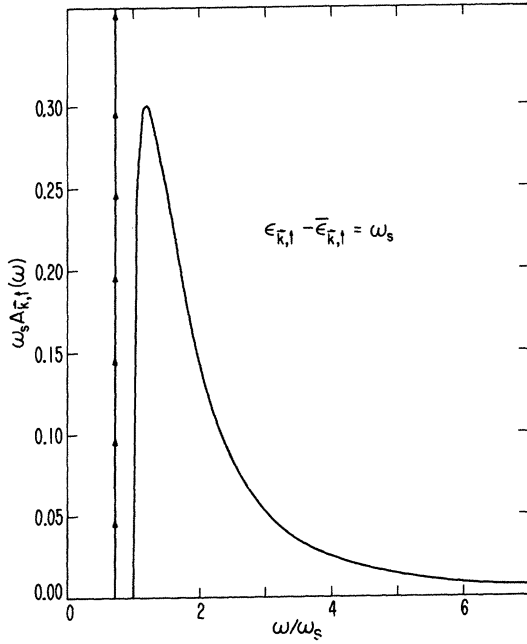


FIG. 1. Plot of the spectral density, as defined by Eq. (4) in the text, against frequency. The parameters contained in the function are $\omega_s = 0.0001$ eV, $c\rho J^2 = 0.00002$ eV, and $D = 5.0$ eV. The zero-frequency shift $\bar{\epsilon}_{k,\uparrow}$ equals 0.000216 eV for these values. This first curve is for kinetic and magnetic energy equal to zero, relative to the shifted origin of energy $\bar{\epsilon}_{k,\uparrow}$. The location of the δ function is dictated by the solution of $\text{Re}G_{k,\uparrow}(\omega)^{-1} = 0$ in the regime where $\omega < \omega_s$.

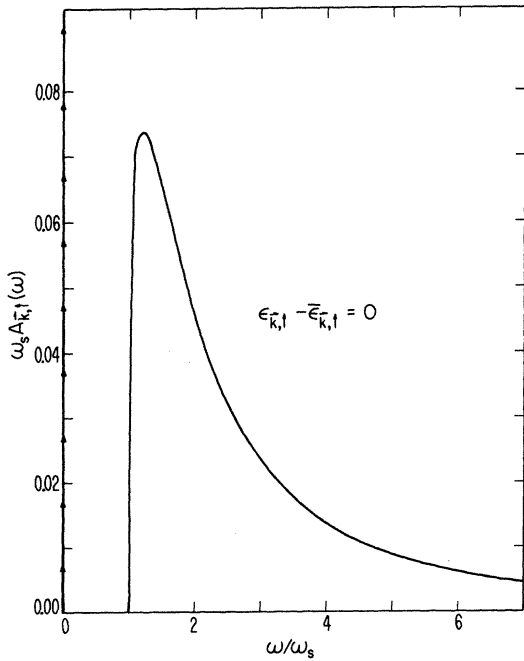


FIG. 2. Plot of the spectral density, as defined by Eq. (4) in the text, against frequency. The parameters are listed in the figure caption for Fig. 1, and the energy excitation $\epsilon_{k,\uparrow} - \bar{\epsilon}_{k,\uparrow}$ is equal to ω_s .

magnetic field:

$$\begin{aligned} \Sigma_{\uparrow}(\omega \pm is) &= c\rho J^2 [\ln |(D + \omega_s - \omega)/(\omega_s - \omega)| \pm i\pi\Theta(\omega - \omega_s)], \\ &\quad (2a) \end{aligned}$$

$$\begin{aligned} \Sigma_{\downarrow}(\omega \pm is) &= c\rho J^2 [\ln |(\omega_s + \omega)/(D + \omega_s + \omega)| \pm i\pi\Theta(-\omega - \omega_s)], \\ &\quad (2b) \end{aligned}$$

where ρ is the one-spin conduction-electron density of states, and where c is the atomic concentration of the

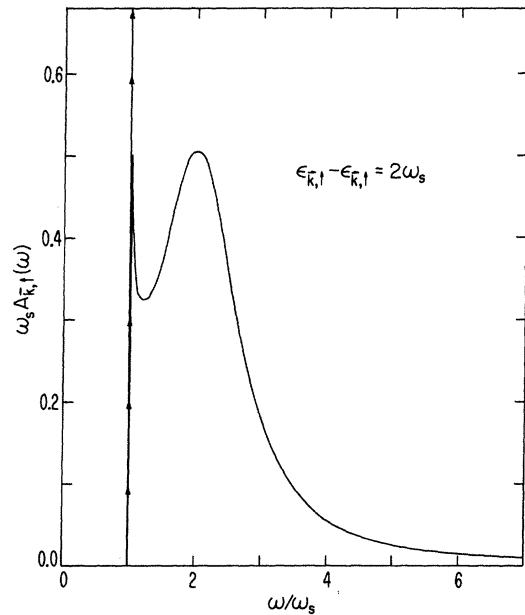


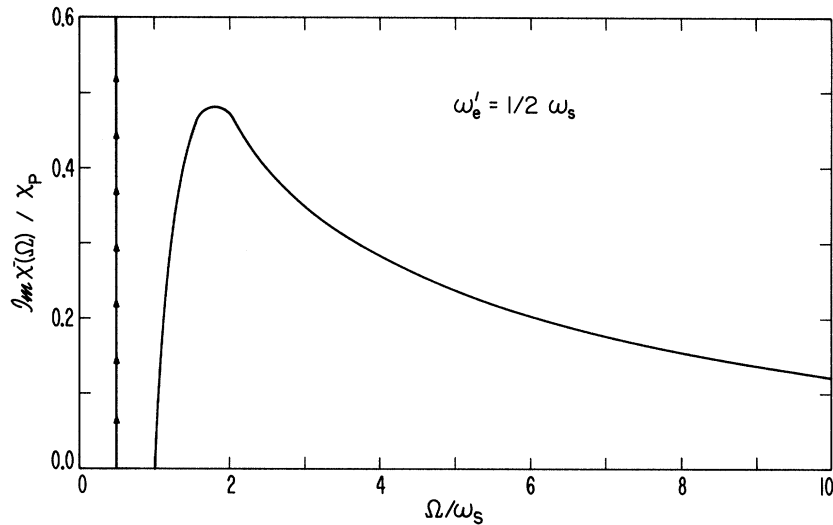
FIG. 3. Plot of the spectral density, as defined by Eq. (4) in the text, against frequency. The parameters are listed in the figure caption for Fig. 1, and the energy excitation $\epsilon_{k,\uparrow} - \bar{\epsilon}_{k,\uparrow}$ is equal to $2\omega_s$.

localized spins. We have used the rectangular-band (width $2D$ centered at the Fermi energy) approximation for the conduction-electron density of states. The relations (2) are interesting, for they enable us to examine the spectral density and hence the validity of the quasiparticle picture.⁶ The propagator for spin- \uparrow electrons is written as

$$\begin{aligned} G_{k,\uparrow}(\omega) &= \{\omega - \epsilon_{k,\uparrow} + i\delta \text{sgn}\omega \\ &\quad + c\rho J^2 [\ln |(D + \omega_s - \omega)/(\omega_s - \omega)| + i\pi\Theta(\omega - \omega_s) \text{sgn}\omega]\}^{-1}, \\ &\quad (3) \end{aligned}$$

with an obvious form for $G_{k,\downarrow}(\omega)$ using (2). We in-

FIG. 4. Plot of the $\text{Im}\chi_e(\Omega)^-$, as defined by (5), using (7), against external frequency Ω . The parameters are the same as those listed in the figure caption of Fig. 1. The conduction-electron exchange-shifted resonance energy ω_e' is equal to $\frac{1}{2}\omega_s$ for this case.



corporate in the Zeeman energies the first-order exchange ("Day") shifts produced by (1).

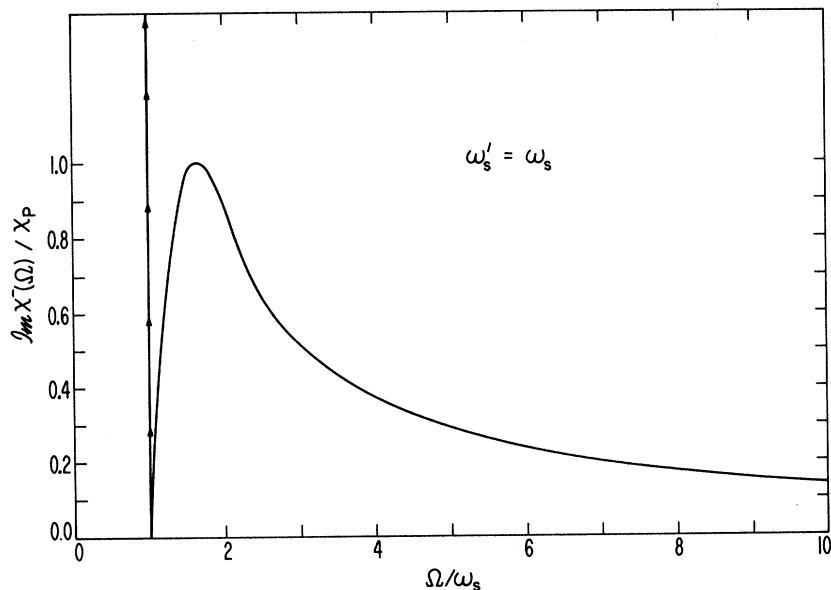
The spectral density appropriate to an electron with wave vector \mathbf{k} and spin \uparrow is

$$A_{\mathbf{k},\uparrow} = (1/\pi) \text{Im}G_{\mathbf{k},\uparrow}(\omega). \quad (4)$$

The form of this quantity as derived from (3) is a δ function at the zero of the real part of the denominator of $G_{\mathbf{k},\uparrow}(\omega)$ for $\omega < \omega_s$, and a smooth structure rising rapidly at $|\omega| = \omega_s + \delta$, where δ is a positive infinitesimal, with a peak (or peaks) which depends (depend) on the frequency ω and the energy $\epsilon_{\mathbf{k},\uparrow}$. At zero frequency, $\text{Re}\Sigma_{\uparrow}$ is nonzero and opposite in sign to $\text{Re}\Sigma_{\downarrow}$, implying a finite shift in the conduction-electron g factor. This shift is just a manifestation of the Kondo

effect in the context of magnetic resonance.⁷ We shall work at magnetic fields which are appropriate to Zeeman energies considerably greater than kT_K , so that the Kondo divergences are not important in the sense of destroying the validity of perturbation theory. The position and area under the δ function depend on the explicit values of $\epsilon_{\mathbf{k},\uparrow}$, $c\rho J^2$, ω_s , and D . Figures 1-3 display (4) for typical values of these parameters. The question of the validity of the quasiparticle picture is very similar to that found by Engelsberg and Schrieffer⁶ for conduction electrons interacting with phonons in an Einstein model, with the important difference that the particle-hole symmetry is absent in the susceptibility problem. The situation appropriate to $A_{\mathbf{k},\downarrow}$ can be derived by simply reversing the sign of ω .

FIG. 5. Plot of the $\text{Im}\chi_e(\Omega)^-$, as defined by (5), using (7), against external frequency Ω . The parameters are the same as those listed in the figure caption of Fig. 1. The conduction-electron exchange-shifted resonance frequency ω_e' is equal to ω_s for this case.



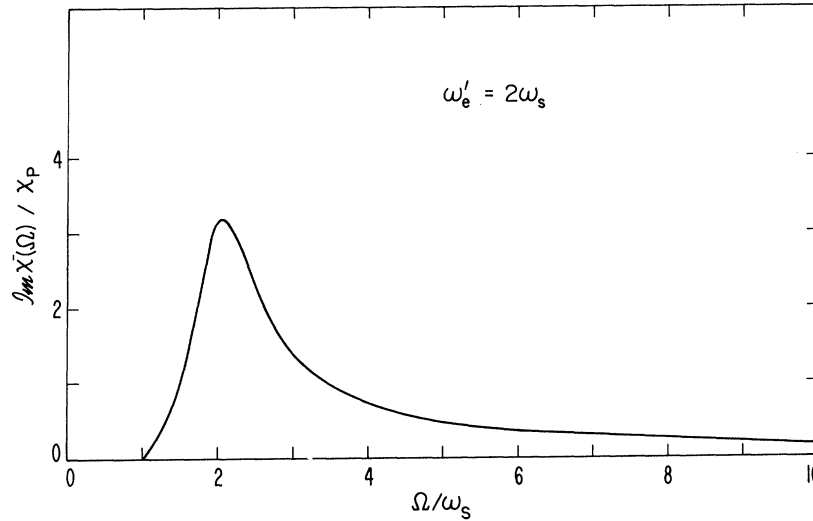


FIG. 6. Plot of the $\text{Im}\chi_e(\Omega)^-$, as defined by (5), using (7), against external frequency Ω . The parameters are the same as those listed in the figure caption of Fig. 1. The conduction-electron exchange-shifted resonance frequency ω_e' is equal to $2\omega_s$ for this case.

The extraordinary frequency dependence of the real and imaginary parts of the self-energies exhibited in (2) makes the direct computation of the transverse dynamic susceptibility considerably more awkward than in previous (high-temperature or decoupling) calculations.⁸ The absence of a wave-vector dependence of the self-energy enables the computation to be carried out analytically, in a manner not unlike that of the generation of the transport equation for an electron gas interacting with phonons.⁹ Two steps are involved. First, using the technique of Fulde and Luther,¹⁰ one can include vertex corrections which are known to influence substantially the final analytic form for the susceptibility. For exchange scattering, however, the second-order vertex correction vanishes at zero temperature (being proportional to $\langle S_z^2 \rangle - \langle S_z \rangle^2$, where S_z is the z component of localized spin), and thus no role will be played by their formal inclusion in our analysis. Second, using (3), an analogous expression for $G_{k,\nu}(\omega)$, and the integration methods of Refs. 9 and 10, we can obtain an expression for the transverse dynamic susceptibility at external frequency Ω . We find

$$\chi_e^-(\Omega) = \chi_P [1 + iJ(\Omega)], \quad (5)$$

where χ_P is the static exchange-enhanced Pauli susceptibility, and

$$J(\Omega) = i \int_{-\Omega}^0 d\omega \left(\Omega - \omega_e + c\rho J^2 \right) \times \ln \left| \frac{(D + \omega_s - \omega - \Omega)(D + \omega_s + \omega)}{(-\omega - \omega_s)(\Omega + \omega - \omega_s)} \right| + 2i\delta + i\pi c\rho J^2 \times [\Theta(-\omega - \omega_s) + \Theta(\Omega + \omega - \omega_s)]^{-1}. \quad (6)$$

This expression is valid to $O(\Omega/E_F)$ and $O(\omega_s/E_F)$, certainly small quantities in our case. The structure of the integral in (6) is very interesting. Consider the following situations.

$\Omega < \omega_s$. In this case, the arguments of the Θ functions never become positive over the region of integration. The imaginary part of $J(\Omega)$ is then a δ function centered at the exchange-shifted value of ω_e . In general, for small $c\rho J^2$ (e.g., in the vicinity of the values used for Figs. 1-3), the logarithm varies little over the frequency integration region since the denominators in the logarithm never become vanishingly small. Comparison with the spectral-density δ -function positions shows that the resonance is shifted by the difference in the real parts of the "up" and "down" self-energies. This difference is manifested as a shift in the g factor. The slow frequency variation of the logarithm in this frequency regime allows us to simply "renormalize" ω_e , the "Day"-shifted conduction-electron resonance frequency. We can then regard the shifted resonance frequency ω_e' as a constant. Thus, in this frequency regime, the transverse dynamic susceptibility of the conduction electrons is centered at the exchange-"dressed" value of ω_e ,

$$\omega_e' \cong \omega_e + c\rho J^2 \ln | D^2 / (\omega + \omega_s)(\omega - \omega_s + \Omega) |.$$

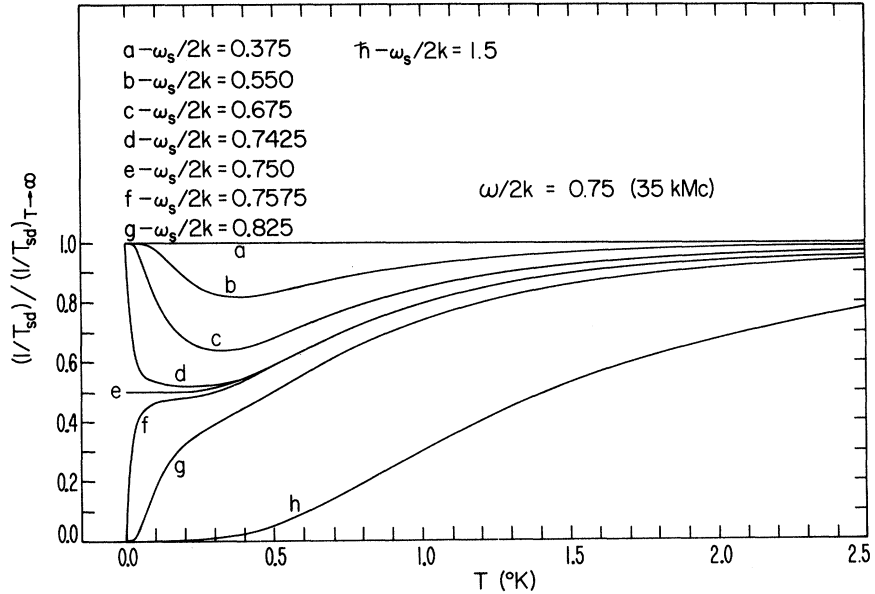
$\Omega > \omega_s$. This regime contains a zero for the argument of both Θ functions, and a concomitant divergence of the logarithm in (6). The zeros occur when

$$\omega = -\omega_s, \quad \omega = \omega_s - \Omega.$$

The coefficient of the logarithm is small (see the values used for Figs. 1-3), so that it becomes substantial only in the immediate vicinity of the zeros. It is at these values of ω that the Θ functions "turn on." The divergence of the real part of the denominator acts only to quench the initial appearance of the Θ functions. In practical terms, this quenching has essentially no effect on the magnitude of the integral, since the logarithm is well behaved and small (indeed, essentially constant) over the remainder of the integration path.

For $\Omega = \omega_s$, the zeros occur only at either end of the integration path, the argument of both Θ functions

FIG. 7. Plot of the vertex-modified decoupling result, Eq. (11), for the conduction-electron spin-resonance linewidth $1/T_{sd}(\Omega)$ as a function of temperature for various values of the Zeeman splitting of the localized spin resonance (i.e., for various values of the localized-spin-resonance g factor). The curves are normalized to the high-temperature value $(8/3)\pi c\rho J^2 S(S+1)$.



remaining negative in the integration region between these points of measure zero. This means that the susceptibility function $J(\Omega)$ remains a δ function at the exchange-dressed value ω_e' . For $\Omega > \omega_s$, the regions of the integration path for which the Θ functions have positive argument increase symmetrically toward one another from either limit. The critical value $\Omega = 2\omega_s$ results in the first Θ function having positive argument for the first half of the integration region and the second Θ function having positive argument for the second half. The integration in (6) produces, therefore, for $\Omega = 2\omega_s$, a symmetric Lorentzian form for the $\text{Re}J(\Omega)$ centered at ω_e' , with width $\pi c\rho J^2$. As Ω continues to increase beyond $2\omega_s$, the integration regions over which the Θ functions have positive argument increase smoothly from zero (at $\Omega = 2\omega_s$) to the full value of Ω (for large Ω). This results in a sum of two Lorentzians, both centered at ω_e' , and with widths $\pi c\rho J^2$ and $2\pi c\rho J^2$. The latter increases in strength (proportional to $\Omega - 2\omega_s$) as Ω increases in magnitude. The strength of the former (proportional to $2\omega_s$) remains constant.

These statements can be made explicit by carrying out the integration contained in (6). We absorb the essentially constant logarithmic term in the resonance frequency, as discussed before, and find

$$0 < \Omega < \omega_s:$$

$$J(\Omega) = i\Omega/(\Omega - \omega_e' + 2i\delta); \quad (7a)$$

$$\omega_s < \Omega < 2\omega_s:$$

$$J(\Omega) = i \left(\frac{2(\Omega - \omega_s)}{\Omega - \omega_e' + i\pi c\rho J^2} + \frac{2\omega_s - \Omega}{\Omega - \omega_e' + 2i\delta} \right); \quad (7b)$$

$$2\omega_s < \Omega:$$

$$J(\Omega) = i \left(\frac{2\omega_s}{\Omega - \omega_e' + i\pi c\rho J^2} + \frac{\Omega - 2\omega_s}{\Omega - \omega_e' + i\pi 2c\rho J^2} \right). \quad (7c)$$

Some graphical examples of $\text{Im}\chi_e^-(\Omega)$, as derived from (5) with the use of (7), are exhibited in Figs. 4–6 for various values of Ω , ω_e' , and ω_s .

III. DISCUSSION

The quantity representing the conduction-electron second-order exchange linewidth is referred to in the literature as $1/T_{sd}$. As seen from (6) and the ensuing discussion, it is very strongly frequency dependent at zero temperature. In particular, it vanishes for frequencies $\Omega < \omega_s$, and its magnitude increases in the range $\omega_s < \Omega < 2\omega_s$, saturating at twice its $\Omega = 2\omega_s$ value when Ω becomes large (but remember that Ω is restricted to be $\ll E_F$).

It is interesting to compare the $T=0$ results of Sec. II with those of Orbach and Spencer. At finite T , they find

$$\text{Im}\Sigma_{\uparrow}(\omega) = \pi c\rho J^2 \{ S(S+1) - \langle S_i^z \rangle^2 + \langle S_i^z \rangle \times \tanh[(\omega_s - \omega)/2kT] \}, \quad (8a)$$

$$\text{Im}\Sigma_{\downarrow}(\omega) = \pi c\rho J^2 \{ S(S+1) - \langle S_i^z \rangle^2 + \langle S_i^z \rangle \times \tanh[(\omega_s + \omega)/2kT] \}. \quad (8b)$$

Here, $\langle S_i^z \rangle \rightarrow -S$ as $T \rightarrow 0$ because ω_s has been taken to be equal to $-g_s H_0^2$. These self-energies are composed of $1/T_2'$ -like contributions from frequency-modulation effects of the localized spin [proportional to $\langle (S_i^z)^2 \rangle - \langle S_i^z \rangle^2$ in (8)] and $1/T_1'$ -like contributions from mutual spin flips of the localized and conduction electrons [remainder of terms in (8)]. As $T \rightarrow 0$, the former vanish and the latter saturate at one of three values, according as ω_s is greater than, lesser than, or equal to ω . In the vanishing- T limit, (8) approximates to

$$\text{Im}\Sigma_{\uparrow}(\omega)|_{T \text{ small}} \cong 2\pi c\rho J^2 S f [(\omega_s - \omega)/kT], \quad (9a)$$

$$\text{Im}\Sigma_{\downarrow}(\omega)|_{T \text{ small}} \cong 2\pi c\rho J^2 S f [(\omega_s + \omega)/kT], \quad (9b)$$

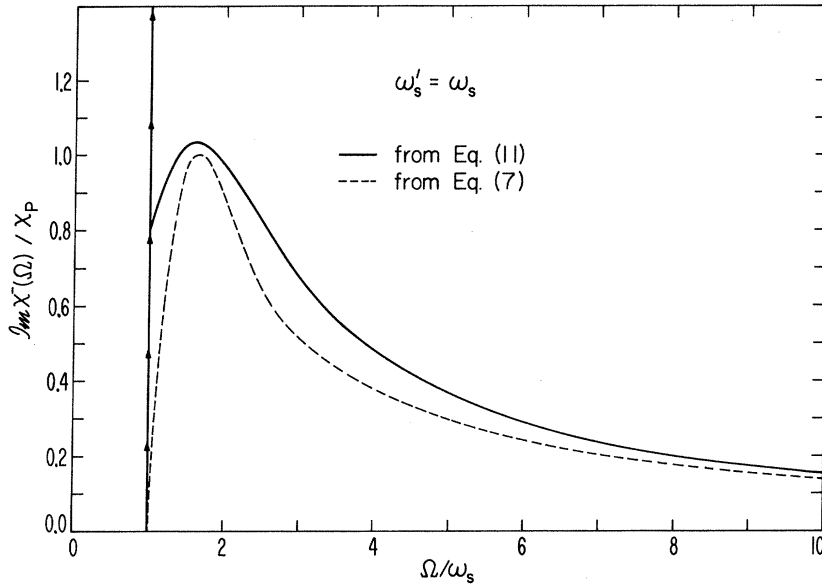


FIG. 8. Comparison of the diagrammatic result for the transverse dynamic conduction-electron resonance absorption (taken from Fig. 5) and that derived using the vertex-modified decoupling linewidth function for $S = \frac{1}{2}$ plotted in Fig. 7 and given by Eq. (11). It is seen that the decoupling result "turns on" sharply when Ω increases beyond ω_s , whereas the diagrammatic result turns on smoothly in the same frequency region. The conduction-electron exchange-shifted resonance frequency ω'_e is equal to ω_s for this figure.

where $f^-(x) = (e^x + 1)^{-1}$. The various limits of (9) are self-evident. For example, $\text{Im}\Sigma_1(\omega)$ vanishes at small T for $\omega_s > \omega$, equals $\pi c \rho J^2 S$ at $\omega_s = \omega$, and is equal to twice that value for $\omega_s < \omega$. We may therefore, in the zero-temperature limit, replace (9) by

$$\text{Im}\Sigma_1(\omega)|_{T=0} = 2\pi c \rho J^2 S \Theta(\omega - \omega_s), \quad (10a)$$

$$\text{Im}\Sigma_1(\omega)|_{T=0} = 2\pi c \rho J^2 S \Theta(-\omega - \omega_s). \quad (10b)$$

For $S = \frac{1}{2}$, Eq. (10) agrees exactly with the zero-temperature diagrammatic $S = \frac{1}{2}$ result (2). As discussed in Orbach and Spencer,² the decoupling procedure results in a transverse-dynamic-susceptibility linewidth which is just the sum of the self-energies (10). When the vertex contribution is added,³ the magnetic-resonance linewidth becomes, at finite temperatures,

$$1/T_{sd} = 2\pi c \rho J^2 \{ 2[\langle (S_i^z)^2 \rangle - \langle S_i^z \rangle^2] + S(S+1) - \langle (S_i^z)^2 \rangle + \langle S_i^z \rangle \tanh \frac{1}{2} \beta (\omega_s - \Omega) \}. \quad (11)$$

The temperature dependence of (11) is plotted in Fig. 7 for Ω in the Q -band regime ($\Omega/2k = 0.75^\circ\text{K}$) for various magnetic field values. At $T=0$, it exhibits a Θ -function behavior, being zero for $\Omega < \omega_s$, one-half its high-temperature value for $\Omega = \omega_s$, and equal to its high-temperature value for $\Omega > \omega_s$. The decoupling result is similar to the exact result (6), but the former "turns on" in an abrupt manner at $\Omega = \omega_s$. The exact result (Figs. 4-6) exhibits a smooth "turn-on" of the Lorentzian breadth. The two results are compared in Fig. 8 for a representative case. Clearly, the decoupling results are crude at $T=0$, but they are all we have at finite temperatures.

The situation concerning an actual magnetic-resonance situation is interesting. In order to break the

so-called bottleneck condition, it is necessary that $\Delta_e \gg 1/T_{sd}(\Omega)$, where Δ_e is the conduction-electron spin-lattice relaxation rate. Failing this, at usual concentrations of localized spins, the primary contribution to the resonance comes from the localized spins with a linewidth sharply reduced from the predicted second-order exchange contribution $1/T_{ds}(\Omega)$. This reduction would not occur if the bottleneck were broken. One can break the bottleneck either by increasing Δ_e or by decreasing $1/T_{sd}(\Omega)$. The latter can be made to occur intrinsically by merely lowering the temperature if $\omega_s > \omega$. Then, on the high-field side of the resonance line, at very low temperatures [see Fig. 7 for an estimate of the magnitudes of T , ω_s , and $1/T_{sd}(\Omega)$ involved] $1/T_{sd}(\Omega) \rightarrow 0$, and the localized spin resonance will be allowed to take on its full linewidth of $1/T_{ds}(\Omega)$ [assuming that ω_e and ω_s are further apart than $1/T_{ds}(\Omega)$ at these temperatures]. This implies a sharp asymmetry in the magnetic-resonance linewidth of dilute transition-metal alloys at low temperatures: A narrow width on the low-field (bottlenecked) side of the resonance and a broad width on the high-field (bottleneck broken) side. Such an asymmetry would allow a direct observation of exchange effects in dilute transition-metal alloys (indeed, even the estimation of J), something which is not possible at normal helium temperatures and usual magnetic fields.

ACKNOWLEDGMENTS

The authors wish to acknowledge very helpful conversations with Professor D. Scalapino and Professor W. Brenig. Professor Scalapino first pointed out to us the similarities between our problem and that treated by Engelsberg and Schrieffer.⁶

* Work supported in part by the National Science Foundation and U.S. Office of Naval Research Contract No. N00014-69-0200-4006.

¹ M. B. Walker, Phys. Rev. B **1**, 3690 (1970).

² H. J. Spencer and R. Orbach, Phys. Rev. **179**, 683 (1969); R. Orbach and H. J. Spencer, *ibid.* **179**, 690 (1969).

³ J. Dupraz, B. Giovannini, R. Orbach, J. D. Riley, and J. Zitkova, in *Proceedings of the International Conference on Electron and Nuclear Magnetic Resonance, Monash University, 1969* (Plenum, New York, 1970), p. 197. Because of an unfortunate error, acknowledgment was not made in this reference to the work of Dr. N. Rivier (private communication). He was responsible for the analytic form for $\chi^-(\omega)$ [Eq. (2.9)] used to discuss the magnetic-resonance bottleneck and should have been included as a coauthor.

⁴ A. A. Abrikosov, Physics **2**, 5 (1965); **2**, 61 (1965).

⁵ H. J. Spencer, Phys. Rev. **171**, 515 (1968).

⁶ An analogous investigation, appropriate to optical-phonon-electron interactions, has been carried out by S. Engelsberg and J. R. Schrieffer, Phys. Rev. **131**, 993 (1963).

⁷ H. J. Spencer and S. Doniach, Phys. Rev. Letters **18**, 994 (1967); Ref. 5 of this paper; D. C. Langreth, D. L. Cowan, and J. W. Wilkins, Solid State Commun. **6**, 131 (1968).

⁸ This is because the high-temperature limits of both the real and imaginary parts of the localized and conduction-electron self-energies are frequency independent. Hence, convolution of the Green's functions to obtain the transverse susceptibility amounts to nothing more than the addition of the imaginary part of the single-particle self-energies when computing the line-width, and the subtraction of the real parts when computing the line shift.

⁹ T. Holstein, Ann. Phys. (N.Y.) **29**, 410 (1964).

¹⁰ P. Fulde and A. Luther, Phys. Rev. **170**, 570 (1968); **175**, 337 (1968).

Faraday Rotation near the Ferromagnetic Critical Temperature of CrBr₃†

JOHN T. HO

Department of Physics and Laboratory for Research in the Structure of Matter, University of Pennsylvania, Philadelphia, Pennsylvania 19104

AND

J. D. LITSTER

Department of Physics and Center for Materials Science and Engineering, Massachusetts Institute of Technology, Cambridge, Massachusetts 02139

(Received 17 July 1970)

We have used the Faraday effect to measure the magnetization of the insulating ferromagnet CrBr₃ as a function of magnetic field (up to 9.5 kG) along 29 isotherms in the temperature range $T_c - 2.8^\circ\text{K} < T < T_c + 6.7^\circ\text{K}$, where $T_c = 32.884^\circ\text{K}$. The numerical results are presented in tabular form. We have also analyzed these data and found that the spontaneous magnetization goes to zero as $(T_c - T)^\beta$ with $\beta = 0.368 \pm 0.005$. Along the critical isotherm $M \sim H^{1/\delta}$ with $\delta = 4.28 \pm 0.1$ and the susceptibility for $M = 0$ and $T > T_c$ diverges as $(T - T_c)^{-\gamma}$ with $\gamma = 1.215 \pm 0.02$. All of the data are consistent with the hypothesis of the static scaling laws. Two simple parametric equations of state were tried, and the better of the two was found to represent the data quite well and be a useful form for calculations of thermodynamic properties in the critical region.

I. INTRODUCTION

The striking similarities in the anomalous behavior of thermodynamic properties near phase transitions in apparently very different materials has led to intense experimental and theoretical interest in the study of magnetic materials, fluids, and other substances in the region around the critical point.¹⁻³

The first general model of the critical point was provided by Landau's theory of second-order phase transitions,⁴ which is equivalent to the Weiss molecular-field model for magnetic systems or to the van der Waals equation for fluids. The Landau model assumes the free energy to be analytic everywhere in the critical region, and predicts thermodynamic anomalies at the critical point which are qualitatively valid but which have been experimentally shown to be quantitatively incorrect. The physical reason for this is clear: The Landau model predicts a diverging susceptibility at the critical point, but fails to include the diverging fluctuations of the order parameter (magnetization) which accompany the rise in susceptibility.

A significant unifying advancement was the concept of static scaling laws⁵⁻⁷ based upon the physical idea that the fluctuations in order parameter could be treated by means of a spatial correlation function with the critical behavior expressed as the divergence of a single correlation length at the critical point. This leads to the mathematical assumption that the free energy is everywhere analytic except at the critical point itself (and possibly along the coexistence curve). Expressed in magnetic language, the static scaling laws may be summarized in the statement that the scaled magnetic field $H | T - T_c |^{-\beta\delta}$ is a function only of the scaled magnetization $M | T - T_c |^{-\beta}$ (where β , δ are the usual critical exponents along the coexistence curve and critical isotherm, respectively). That is,

$$H | T - T_c |^{\beta\delta} = \Phi(M | T - T_c |^\beta). \quad (1)$$

These ideas were first experimentally tested and verified within the accuracy of available data for the metallic ferromagnets nickel^{8,9} and CrO₂ (only for $T > T_c$).¹⁰ The analysis of data collected by Green,